Adaptive sliding mode control of a four-wheel-steering autonomous vehicle with uncertainty using parallel orientation and position control

Armin Norouzi*, Hadi Adibi-Asl, Reza Kazemi, Parvin Fathi Hafshejani

Faculty of Mechanical Engineering
K.N. Toosi University of Technology
Vanak Square, Molla-Sadra, Pardis, Tehran 19697, Iran
Email: anorouzi@mail.kntu.ac.ir
Email: hadibi@kntu.ac.ir
Email: kazemi@kntu.ac.ir
Email: pfathi@mail.kntu.ac.ir
*Corresponding author

Abstract

Control Systems of autonomous vehicles or Driver Assistant Control Systems always face uncertainties due to the in-vehicle and environmental disturbances. In addition, the steering ability for rear tires leads to more stability and more handling and maneuverability. In this paper the adaptive sliding mode control (ASME) strategy is employed to improve handling issues due to the road's friction, which plays a key role in handling dynamics. . The proposed dynamic model used in this paper is simple and useful two-degree of freedom model. In this paper, two parallel ASMCs are used: one for positioning error and the other for angular error. The simulation are executed for two different road conditions with considering the hypercritical condition. To verify the designed controller, the controller is applied to the non-linear full vehicle model. The simulation results prove that the controller perfectly works for different road conditions. The controller is also robust against uncertainties such as road friction.

Keywords: Autonomous Vehicle, Four-Wheel-Steering Vehicle, Vehicle Lateral Control, Adaptive Sliding Model Control

Biographical notes: Armin Norouzi received his B.S. (2014) in mechanical engineering from University of Tabriz (Tabriz, Iran) and the M.S. (2017) in Mechanical Engineering/vehicle dynamics & control from K.N.Toosi University of technology (Tehran, Iran). His research interests include Vehicle Dynamic Systems, Nonlinear Control and Autonomous Vehicle.

Hadi Adibi-Asl received his B.S. (2007) in Mechanical Engineering from Amirkabir University of Technology (Tehran, Iran) and an M.S. (2009) in Mechanical Engineering from Memorial University of NL (St. John's, Canada) and a PhD (2015) in Mechanical Engineering from University of Waterloo (Waterloo, Canada). He is faculty member of K. N. Toosi University of Technology (2015, up to present). His research interests include Mathematical Modelling, Dynamics and Control and Vehicle Dynamics & Control.

Reza Kazemi received his B.S. (1993) and M.S. (1995) in Mechanical Engineering from Isfahan University of Technology (Isfahan, Iran) and a PhD (2000) in Mechanical Engineering from Amirkabir University of Technology (Tehran, Iran). He is faculty member of K. N. Toosi University of Technology (2001, up to present). His research interests include Vehicle Dynamic Systems, Automotive Chasis Design and Nonlinear Dynamics systems.

Parvin Fathi Hafshejani received his B.S. (2014) in mechanical engineering from Esfahan University of Technology (Esfahan-Iran) and the M.S. (2017) in Mechanical Engineering from K.N.Toosi University of technology (Tehran-Iran). Her research interests include nondestructive evaluation and Vehicle Dynamic Systems.

1. Introduction

Autonomous vehicles, which is recently the subject of research and development of many well-known car companies, is a driverless vehicle in which properties of traditional vehicles are preserved. Taking advantages of some technologies such as Lidar, GPS, radar and computer vision, autonomous vehicles can sense the environment. Vehicle's control system interprets the obtained data and regarding the possible obstacles and street signs, navigates the vehicle in an appropriate path. One of the major problems in this field is the safet and security issues, particularly in diverse weather conditions. The vehicle should be able to retain its stability in any environmental condition.

One approach for increasing the stability and enhancing the handling and maneuverability of vehicle is to use Four Wheel Steering (4WS) [1]. Rear steering in for 4WS will result in two control inputs (rear and front steering angle). Adding rear steering broadens the ranges of choices in designing the controller. In other words, in vehicles with one input for the controller, position and orientation errors should be eliminated, but in the case of 4WS vehicles, one controller is assigned for position error and another one for orientation error.

Researchers have shown that the closed loop control design can significantly enhance the stability of 4WS vehicles. They have used numerous control rules in designing a 4WS vehicle. The authors of [2] have used optimal control rule to navigate the vehicle, and five models to establish the relationship between rear and front steering angle. In this models, rear steering angle can be proportionally related to front steering angle. In the model, the rear steering angle functions depending on front steering angle, longitudinal velocity, and yaw rate. In another model, rear steering angle is independent of front steering angle. In addition to [2] in which the optimal control rule is used, authors of [3] [4], and [5] have also taken the advantages of this rule. Moreover, [6] is used an optimal controller for yaw momentum and rear steering angle for 4WS. The designed control rule in [6] is effective in handling stability enhancement. However, the gain of steady state of yaw rate depends on the steering angle applied by the driver. Thus, the gain decreases in higher velocities. Consequently, understeering occurs and the responsibilities of driver increases. Due to the limitations of optimal controllers, [7-9], the optimal controller is integrated with robust controllers $H\infty$ to achieve a better performance, particularly in higher velocities. The authors of [10] have also used IMC technique based on optimal controller $H\infty$ and achieved more satisfying results.

Regardless of many issues, due to their better response and simpler implementation in empirical systems, PID controllers have attracted much interests. Fuzzification [11] and adaptation [12] of PID controller's coefficients will simply result in a non-linear behavior in the controller. References [13], [14], and [15] have used a PI to control a 4WS among which the controller used in [13] is non-linear.

The authors of [16] have controlled yaw angle in a 4WS using fuzzy logics. Moreover, [17] has used two fuzzy controllers to monitor the side slip angle and yaw rate. The authors of [18] have controlled a 4WS using a neural fuzzy system and genetic algorithm. The use of an optimization algorithm in this fuzzy controller have yielded more satisfying results such as more accurate path tracking.

Due to the changes of system parameters over time and some unknown parameters, using adaptive and robust control rules has better response in vehicles. Wakamatsu et al. [19] and Shiotsuka et al. [20] have used a feedback and feed-forward controller and the friction coefficient between tires and vehicle to design an adaptive controller for 4WS vehicles. Shiotsuka et al. [20] have also used the artificial neural networks to train a system to generate cornering forces of tires. The inputs of this system are velocity and friction coefficient between tires and the road. The authors of [21-24] have developed control systems that are robust against parameter changes and external disturbances such as crosswinds. In [23], a vehicle model with parameters that vary with time has been used. The longitudinal velocity in different times is provided to the system by a controller and, then, the model parameters change.

Another method of designing robust controllers is to use sliding mode controllers that is able to control the system under uncertainties and external disturbances. Tires' lateral stiffness, the friction between tires and the road, and disturbances such as crosswinds and robustness against different maneuvers are usually considered in sliding mode controllers for 4WS vehicles [25-32]. Reference [24] has integrated a state-feedback and a sliding mode controller using fuzzy rules. Reference [30] has used a fractional order sliding mode controller. The results of that research shows more system stability. Reference [33] has used an adaptive fuzzy sliding mode controller with Fuzzy Boundary Layer for controlling a 2WS autonomous vehicle. The authors of [31] and [32] have designed a fault-tolerant control using sliding mode controller. Reference [34] has used a non-linear model predictive control (MPC) to control a 4WS vehicle. In addition, some researchers have used the decoupling to design a controller independent of any motion [14, 15, 24, 35-37].

In this paper, using two parallel controllers, the position and the angle of vehicle with respect to desired path as input are simultaneously controlled. In the next section, the dynamic model has been presented and the dynamic model based on position and angle errors is obtained. Then, controlling strategy and parallel adaptive sliding mode controllers are designed. In section 3, the definition of Lyapunov function and stability criteria, and the stability of adaptive controllers are studied. In section 4, the response of the system in different weather conditions in a sinusoidal maneuver is simulated. To simulate the proposed controller, the non-linear full vehicle model is employed.

2. Modeling

2.1. The bicycle model

In this paper, a simplified 2 degree-of-freedom vehicle model, which is known as bicycle model, is used for control development as shown in Figure 1. The model has two state variables such as yaw rate and sideslip angle.

[Insert Figure 1]

Assuming the longitudinal velocity of vehicle to be constant, and neglecting the roll, pitch, and bounce effects, the model can be obtained from the lateral dynamic equations as presented in Eq. 1 [38].The parameters of model are also listed in Table 1.

$$\dot{\beta} = \left(-2\mu\frac{c_f+c_r}{mV_x}\right)\beta + \left(-1+2\mu\frac{l_rc_r-l_rc_r}{mV_x{}^2}\right)r + (2\mu\frac{c_f}{mV_x})\delta_f + (2\mu\frac{c_f}{mV_x})\delta_r$$
$$\dot{r} = (2\mu\frac{l_rc_r-l_rc_r}{J})\beta + (-2\mu\frac{c_fl_f^2+c_rl_r^2}{JV_x})r + (2\mu\frac{l_fc_f}{J})\delta_f + (-2\mu\frac{l_rc_r}{J})\delta_r \quad (1)$$

[Insert Table 1]

The linear tire model has been used in this dynamic vehicle model. The lateral tire forces are shown in the following equation.

$$F_f = \alpha_f c_f^* = \alpha_f c_f \mu$$
$$F_f = \alpha_r c_r^* = \alpha_r c_r \mu \quad (2)$$

where α is sideslip angle, c^* is the nominal stiffness of tires, and μ is coefficient of friction. Taking into account the relationship between lateral velocity of vehicle and sideslip angle (Eq. 3), and the fact that yaw rate of vehicle is equal to derivation of yaw (Eq. 4), one can apply Eq.3 and Eq. 4 to Eq. 1 to obtain the bicycle model of vehicle with lateral position and yaw angle as degrees of freedom (Eq. 5).

$$\beta = \frac{\dot{y}}{V_x} \quad (3)$$

$$r = \dot{\psi} \quad (4)$$

$$\ddot{y} = (-2\mu\frac{c_f+c_r}{mV_x})\dot{y} + (-V_x + 2\mu\frac{l_rc_r-l_fc_f}{mV_x})\dot{\psi} + (2\mu\frac{c_f}{m})\delta_f + (2\mu\frac{r}{m})\delta_r$$
$$\ddot{\psi} = (2\mu\frac{l_rc_r-l_fc_f}{JV_x})\dot{y} + (-2\mu\frac{c_fl_f^2+c_rl_r^2}{JV_x})\dot{\psi} + (2\mu\frac{l_fc_f}{J})\delta_f + (-2\mu\frac{l_rc_r}{J})\delta_r \quad (5)$$

The vehicle model is subjected to some uncertainties, so the controller must be robust to achieve a much better performance. One of the most important uncertainties that affects both stability and handling is the coefficient of friction between tires and surface of the road. The value of coefficient of friction for different environmental conditions is shown in Table 2. The minimum and maximum values of friction coefficient studied in this paper are 0.01 and 1, respectively. All coefficients of dynamic model are defined, based on these uncertainties, in Appendices I and II. Moreover, for the purpose of simulation, the average value of dry and icy road friction has been

used. For more feasibility of simulation of dry road, the friction coefficient was considered equal to one.

[Insert Table 2]

2.2. Vehicle model based on position and orientation error

To study the dynamic behavior of vehicle and to design controller, it is more suitable that the dynamic equations be given in the form of a function of position and orientation error with respect to the road. Lateral position and orientation errors are schematically shown in Figure 2 and are defined as follows [39]:

$\boldsymbol{e_1}$ the distance of the C.G. of the vehicle from the center line of the lane

$\boldsymbol{e_2}$ the orientation error of the vehicle with respect to the road

[Insert Figure 2]

The relationships between the errors and the model's degrees of freedom is explained by the following equation [39]:

$$\dot{e}_1 = \dot{y} + V_x(\psi - \psi_d) = V_x(\beta + \psi - \psi_d)$$
$$e_2 = \psi - \psi_d \tag{6}$$

Using equations 5 and 6, dynamic equations of 4WS vehicle as a function of position and orientation errors is obtained.

$$\ddot{e}_1 = a_{11}\dot{e}_1 + a_{12}e_2 + a_{13}\dot{e}_2 + b_{11}\delta_f + b_{12}\delta_r + d_1\dot{\psi}_d$$
$$\ddot{e}_2 = a_{21}\dot{e}_1 + a_{22}e_2 + a_{23}\dot{e}_2 + b_{21}\delta_f + b_{22}\delta_r + d_2\dot{\psi}_d - \ddot{\psi}_d \tag{7}$$

where the value of coefficients are given in Appendix I. The input of this model with respect to global coordinates is defined as follows [39]:

$$X_{des} = \int_0^t V_x \cos(\psi_d)\, dt$$
$$Y_{des} = \int_0^t V_x \sin(\psi_d)\, dt \tag{8}$$

As shown in Figure 2, the desired yaw rate is equal to the slope of the road function. Since yaw angle is small, x_{des} is considered to be equal to V_x.

$$\psi_d = \tan^{-1}\frac{\dot{Y}_{des}}{\dot{X}_{des}} \approx \frac{\dot{Y}_{des}(t)}{V_x} \tag{9}$$

And finally the output as a function of global coordinates is yielded and is given in reference [39].

$$X = X_{des} - e_1 sin(\psi)$$
$$Y = Y_{des} + e_1 cos(\psi) \tag{10}$$

3. Controller design

Sliding mode controller is a proper controller in confronting the uncertainties of controlling system of autonomous vehicles. It has some advantages, such as good performance when there exist un-modeled dynamics, non-sensitivity to parameter changes, excluding the external disturbances, and fast dynamic response [40]. Typically, this controller is used when there exist uncertainties in nonlinear systems. In this method of controller design, the range of uncertainty of parameters should be known. In fact, the tracking problem in an n-order system is converted to a one dimensional sliding surface stability problem. The main challenge of this method is chattering phenomenon, which is resolved by defining a suitable boundary layer [41]. The objective of this section is to design the sliding mode controller based on the dynamic system shown in Eq. 7. The controller strategy used in this article is shown in the block diagram of Figure 3.

As shown in the Figure 3,, two adaptive sliding mode controllers are used in a parallel manner. One of them is responsible to eliminate the orientation error using rear steering control input to make the yaw angle of vehicle equal to the desired yaw angle of input. The other controller is responsible to eliminate the position error using front steering control input to navigate the vehicle on the input path. When these errors are simultaneously eliminated, the final output of vehicle should completely track the input path.

[Insert Figure 3]

3.1. ASMC controller design for position error

Since the system is of 2 DOF, sliding surface is selected as follows:

$$s_1 = \left(\frac{d}{dt} + \lambda_1\right)\tilde{x}_1 = \dot{e}_1 + \lambda_1 e_1 \tag{11}$$

where λ_1 is positive, and $\tilde{x}_1$ is the position error.

$$\tilde{\boldsymbol{x}}_{\mathbf{1}} = \boldsymbol{e}_{\mathbf{1}} \tag{12}$$

Differentiating sliding surface yields

$$\dot{s}_1 = (\hat{a}_{11} + \lambda_1)\dot{e}_1 + \hat{a}_{12}e_2 + \hat{a}_{13}\dot{e}_2 + \hat{b}_{11}u_f + \hat{b}_{12}u_r + \hat{d}_1\dot{\psi}_d \tag{13}$$

where u_f and u_r are rear (δ_r) and front (δ_f) steering angle. According to Reference [41], the best controlling rule for the position error is yielded from $\dot{s} = 0$. Therefore, putting $\dot{s}_1$ equal to zero, the best controlling rule is obtained as

$$u_{feq} = -\hat{b}_{11}^{-1}(\hat{u}_1) \tag{14}$$

where $\hat{u}_1$ is defined as

$$\hat{u}_1 = \hat{A}_{11}\dot{e}_1 + \hat{a}_{12}e_2 + \hat{a}_{13}\dot{e}_2 + \hat{b}_{12}u_r + \hat{d}_1\dot{\psi}_d \tag{15}$$

According to Reference [41], the sliding criterion is as follows

$$\frac{1}{2}\frac{d}{dt}s_1^2(t) \le \eta_1|s_1(t)| \tag{16}$$

To satisfy this equation, the extra term is added to the u_{feq} as shown in Eq. 17..

$$u_f = u_{feq} - k_1 \hat{b}_{11}^{-1} \text{sign}(s_1) \tag{17}$$

The bounds of k_1 is provided in Reference [41] as

$$k_1 > \gamma(F_1 + \eta_1) + (\gamma - 1)|\hat{u}_1| \tag{18}$$

F_1 is defined as

$$\left|f_1^+ - \hat{f}_1\right| \leq F_1 \tag{19}$$

$\hat{f}_1$ is an approximation of f_1. In fact, the upper bound of this approximation has been limited by F_1. The relationships for f_1, $\hat{f}_1$, and F_1 are presented in Appendix II.

In order to eliminate the chattering, saturate function is used, instead of Sign function. Saturate function is provided in Equation 20 and is shown in Figure 4.

$$\text{sat}\left(\frac{s}{\varphi}\right) = \begin{cases} 1 & \frac{s}{\varphi} > 1 \\ \frac{s}{\varphi} & -1 < \frac{s}{\varphi} < 1 \\ -1 & \frac{s}{\varphi} < -1 \end{cases} \tag{20}$$

[Insert Figure 4]

Finally, the equation for SMC controller is obtained as

$$u_f = u_{feq} - k_1 \hat{b}_{11}^{-1} sat\left(\frac{s_1}{\varphi_1}\right) \tag{21}$$

Although there are several advantages in using sliding mode controller, but in needs to know the upper and lower bounds of uncertainties to compute the switching gain. Thus, to avoid the computation of the upper bound of uncertainties, an adaptive rule for computation of sliding or switching gain is presented here. For this purpose, controlling signal is rewritten as [42]:

$$u_{fASMC} = u_{feq} - \hat{\theta}_1 \Omega_1 \hat{b}_{11}^{-1} \text{sat}\left(\frac{s_1}{\varphi_1}\right) \tag{22}$$

where $\hat{\theta}_1$ is switching gain and is updated using the following formula.

$$\dot{\hat{\theta}}_1(t) = \Omega_1 |s_1(t)| \tag{23}$$

$$\hat{\theta}_1(0) = 0$$

where Ω_1 is positive and constant. This constant allows us to select the adaptive velocity in an arbitrary manner. There are, however, some constraints which will be addressed in the proper part.

3.2. ASMC controller design for orientation error

Considering the fact that the system is of 2 degrees of freedom, the sliding surface is chosen as

$$s_2 = \left(\frac{d}{dt} + \lambda_2\right) \tilde{x}_2 = \dot{e}_2 + \lambda_1 e_2 \tag{24}$$

where λ_2 is positive and $\tilde{x}_2$ is the position error

$$\tilde{x}_2 = e_2 \tag{25}$$

Differentiating from the sliding surface, we have

$$\dot{s}_1 = \hat{a}_{21}\dot{e}_1 + \hat{a}_{22}e_2 + (\hat{a}_{23} + \lambda_2)\dot{e}_2 + \hat{b}_{21}u_f + \hat{b}_{22}u_r + \hat{d}_2\dot{\psi}_d \tag{26}$$

Similar to the previous controller, the best control is achieved when Eq.26 is set equal to zero.

$$u_{req} = -\hat{b}_{22}^{-1}(\hat{u}_2) \tag{27}$$

where $\hat{u}_1$ is expressed as

$$\hat{u}_2 = \hat{a}_{21}\dot{e}_1 + \hat{a}_{22}e_2 + \hat{A}_{23}\dot{e}_2 + \hat{b}_{21}u_f + \hat{d}_2\dot{\psi}_d \tag{28}$$

According to Reference [41], the sliding surface is defined as

$$\frac{1}{2}\frac{d}{dt}s_2^2(t) \le \eta_2|s_2(t)| \tag{29}$$

A term will be added to u_{feq} to satisfy this condition.

$$u_r = u_{req} - k_2\hat{b}_{22}^{-1}\text{sign}(s_2) \tag{30}$$

The bounds of k_2 is obtained as

$$k_2 > \gamma(F_2 + \eta_2) + (\gamma - 1)|\hat{u}_2| \tag{31}$$

and similar to previous controller, F_2 is defined as

$$\left|f_2^+ - \hat{f}_2\right| \le F_2 \tag{32}$$

The relationships between f_2 ,$\hat{f}_2$ and F_2 are presented in Appendix II.

In order to eliminate the chattering, Sat function and boundary layer is used. Therefore, the final SMC control signal is obtained as

$$u_r = u_{req} - k_2\hat{b}_{22}^{-1}\text{sat}(\frac{s_2}{\varphi_2}) \tag{33}$$

Again, adaptive controller rule is applied, and the control signal (22) is rewritten as

$$u_{rASMC} = u_{req} - \hat{\theta}_2\Omega_2\hat{b}_{22}^{-1}\text{sat}(\frac{s_2}{\varphi_2}) \tag{34}$$

where $\hat{\theta}_2$ is switching gain and is updated using

$$\begin{aligned}\dot{\hat{\theta}}_2(t) &= \Omega_2|s_2(t)| \\ \hat{\theta}_2(0) &= 0\end{aligned} \tag{35}$$

where Ω_2 is a constant. This constant helps in choosing the adaptive velocity for switching gain arbitrarily. However, there are, again, some constraints, which are addressed in Section 4.

4. Stability Analysis of the Designed ASMC Controller

4.1. Stability Analysis of position error controller

To analyze the controller designed for position error, the candidate Lyapunov function is chosen as

$$V_1 = \frac{1}{2}s_1^2 + \frac{b_{11}\hat{b}_{11}^{-1}}{2}\tilde{\theta}_1^2 \tag{36}$$

where $\tilde{\theta}_1$ is defined as

$$\tilde{\theta}_1 = \hat{\theta}_1 - \theta_1 \tag{37}$$

and θ_1 is equal to k_1 obtained from the SMC controller

$$\theta_1 = k_1 \geq \gamma(F_1 + \eta_1) + (\gamma - 1)|\hat{u}_1| \tag{38}$$

To analyze the Lyapunov stability, the candidate Lyapunov function is differentiated

$$\dot{V}_1 = s_1\dot{s}_1 + b_{11}\hat{b}_{11}^{-1}\tilde{\theta}_1\dot{\tilde{\theta}}_1$$

$$= s_1\big(A_{11}\dot{e}_1 + a_{12}e_2 + a_{13}\dot{e}_2 + b_{11}\big(-\hat{b}_{11}^{-1}\big)\{\hat{A}_{11}\dot{e}_1 + \hat{a}_{12}e_2 + \hat{a}_{13}\dot{e}_2 + \hat{b}_{12}u_r + \hat{d}_1\dot{\psi}_d + \hat{\theta}_1\Omega_1 \text{sign}(s_1)\} + b_{12}u_r + d_1\dot{\psi}_d\big) + b_{11}\hat{b}_{11}^{-1}(\hat{\theta}_1 - \theta_1)\Omega_1|s_1(t)|$$

$$\leq \big|\bar{A}_{11}\dot{e}_1 + \bar{a}_{12}e_2 + \bar{a}_{13}\dot{e}_2 + \bar{b}_{12}u_r + \bar{d}_1\dot{\psi}_d\big||s_1(t)| + \big|1 - b_{11}\hat{b}_{11}^{-1}\big||\hat{u}_1||s_1(t)| - b_{11}\hat{b}_{11}^{-1}\hat{\theta}_1\Omega_1|s_1(t)| + b_{11}\hat{b}_{11}^{-1}\hat{\theta}_1\Omega_1|s_1(t)| - b_{11}\hat{b}_{11}^{-1}\theta_1\Omega_1|s_1(t)|$$

using Appendix II, we have

$$\dot{V}_1 \leq F_1|s_1(t)| + |1-\gamma^{-1}||\hat{u}_1||s_1(t)| - \gamma^{-1}(\gamma(F_1 + \eta_1) + (\gamma - 1)|\hat{u}_1|)\Omega_1|s_1(t)|$$

$$\dot{V}_1 \leq (1 - \Omega_1)(F_1 + |1-\gamma^{-1}||\hat{u}_1|)|s_1(t)| - \eta_1\Omega_1|s_1(t)|$$

Since η_1 is positive, the above inequality is satisfied, only when Ω_1 is larger than 1. Therefore, we have

$$\Omega_1 \geq 1 \quad \rightarrow \quad \dot{V}_1 \leq 0 \tag{39}$$

4.2. Stability Analysis of Orientation Error Controller

The Lyapunov function for this controller is similar to the previous section. That is

$$V_2 = \frac{1}{2}s_2^2 + \frac{b_{22}\hat{b}_{22}^{-1}}{2}\tilde{\theta}_2^2 \tag{40}$$

where $\tilde{\theta}_2$ is defined as

$$\tilde{\theta}_2 = \hat{\theta}_2 - \theta_2 \tag{41}$$

and θ_2 is equal to k_2 obtained from the SMC controller.

$$\theta_2 = k_2 \geq \gamma(F_2 + \eta_2) + (\gamma - 1)|\hat{u}_2| \tag{42}$$

To analyze the Lyapunov stability, the candidate Lyapunov function is differentiated

$$\dot{V}_2 = s_2\dot{s}_2 + b_{22}\hat{b}_{22}^{-1}\tilde{\theta}_2\dot{\tilde{\theta}}_2$$

$$= s_2\big(a_{21}\dot{e}_1 + a_{22}e_2 + A_{23}\dot{e}_2 + b_{22}\big(-\hat{b}_{22}^{-1}\big)\{\hat{a}_{21}\dot{e}_1 + \hat{a}_{22}e_2 + \hat{A}_{23}\dot{e}_2 + \hat{b}_{21}u_f + \hat{d}_2\dot{\psi}_d + \hat{\theta}_2\Omega_2 sign(s_2)\} + b_{21}u_f + d_2\dot{\psi}_d\big) + b_{22}\hat{b}_{22}^{-1}(\hat{\theta}_2 - \theta_2)\Omega_2|s_2(t)|$$

$$\leq \big|\bar{a}_{21}\dot{e}_1 + \bar{a}_{22}e_2 + \bar{A}_{23}\dot{e}_2 + \bar{b}_{21}u_f + \bar{d}_2\dot{\psi}_d\big||s_2(t)| + \big|1 - b_{22}\hat{b}_{22}^{-1}\big||\hat{u}_2||s_2(t)| - b_{22}\hat{b}_{22}^{-1}\hat{\theta}_2\Omega_2|s_2(t)| + b_{22}\hat{b}_{22}^{-1}\hat{\theta}_2\Omega_2|s_2(t)| - b_{22}\hat{b}_{22}^{-1}\theta_2\Omega_2|s_2(t)|$$

Using Appendix II, we have

$$\dot{V}_2 \leq F_2|s_2(t)| + |1-\gamma^{-1}||\hat{u}_2||s_2(t)| - \gamma^{-1}(\gamma(F_2 + \eta_2) + (\gamma - 1)|\hat{u}_2|)\Omega_1|s_2(t)|$$

$$\dot{V}_1 \leq (1 - \Omega_2)(F_2 + |1-\gamma^{-1}||\hat{u}_2|)|s_2(t)| - \eta_2\Omega_2|s_2(t)|$$

Since η_1 is positive, the above inequality is satisfied, only when Ω_1 is larger than 1. Therefore, we have

$$\Omega_2 \geq 1 \quad \rightarrow \quad \dot{V}_2 \leq 0 \tag{43}$$

5. Results and Discussion

Generally, the controller output signals that are rear and front steering angles was designed as follows

$$s_1 = \dot{e}_1 + \lambda_1 e_1$$

$$u_{fASMC} = -\hat{b}_{11}^{-1}\big(\hat{A}_{11}\dot{e}_1 + \hat{a}_{12}e_2 + \hat{a}_{13}\dot{e}_2 + \hat{b}_{12}u_r + \hat{d}_1\dot{\psi}_d\big) - \hat{\theta}_1\Omega_1\hat{b}_{11}^{-1}sat(\frac{s_1}{\varphi_1})$$

$$\dot{\hat{\theta}}_1(t) = \Omega_1|s_1(t)|$$

$$\hat{\theta}_1(0) = 0$$

$$s_2 = \dot{e}_2 + \lambda_2 e_2$$

$$u_{rASMC} = -\hat{b}_{22}^{-1}\big(\hat{a}_{21}\dot{e}_1 + \hat{a}_{22}e_2 + \hat{A}_{23}\dot{e}_2 + \hat{b}_{21}u_f + \hat{d}_2\dot{\psi}_d\big) - \hat{\theta}_2\Omega_2\hat{b}_{22}^{-1}sat(\frac{s_2}{\varphi_2})$$

$$\dot{\hat{\theta}}_2(t) = \Omega_2|s_2(t)|$$

$$\hat{\theta}_2(0) = 0$$

where λ_1 ،Ω_1 ،λ_2 و Ω_2 are adjustable controller design parameters. In addition, λ coefficients are larger than zero, and Ω coefficients are larger than 1 and determine the adaption velocity.
The input maneuver is sinusoidal and we have

$$y_{ref}(t) = \begin{cases} 0 & 0 < t \leq \frac{\pi}{2} \\ W\ sin(t) & \frac{\pi}{2} < t \leq \frac{7\pi}{2} \\ 0 & t > \frac{7\pi}{2} \end{cases} \quad (44)$$

where W is equal to 3.74 (the width of each lane). The sinusoidal curvature of the maneuver has been plotted in Figure 5.

[Insert Figure 5]

With applying this input, obtaining the suitable input yaw rate, and considering the block diagram shown in Figure 3, it is possible to obtain the output of the system for two different weather conditions and a velocity of 40 m/s based on the designed controller. The equations of motion in the CarSim math models are valid for full nonlinear 3D motions of rigid bodies. It is not required to know the details of the linkages and gears in the suspensions and steering, hence, reducing the amount of information needed to obtain accurate predictions. The components that have significant effect on handling, braking, and acceleration are represented with nonlinear tables of measurable data. Figure 6 illustrate the output of the system for two different road frictions (μ = 0.1,1). Inset (a), in figure 6, indicates the vehicle's path and the reference path. Insets (b) and (c), in figure 6, indicate the yaw angle and lateral position errors. Insets (d) and (e), respectively, indicate the sliding surface of two parallel ASMC controllers. Insets (f)-(i) show vehicle side slip angle, yaw rate, and yaw and roll angle. Also, Insets (j) and (k), respectively, indicate the rear and front steering angle as outputs of the controller for fictions μ = 1 and μ = 0.1.

As it is shown in Inset (a) of Figure 6, in the case of a friction equal to one, the vehicle perfectly tracks the desired path. This prefect tracking can be induced from the low value of lateral position (b) and orientation errors (c). For icy road with friction value of 0.1, the system shows acceptable tracking. The vehicle only deviates from the path at its maximum curvatures. As it can be seen from Inset (c), the orientation error has variations which result in deviations of vehicle from the desired path. However, since the error range is short (0.2 degree), this issue is not significant in path tracking. Insets (d) and (e) show that both sliding surfaces, in the absence of chattering, converge to zero. The range of these surfaces is higher for lower frictions. In regard to appropriate performance of the controller in each friction coefficient, the side slip, yaw, and roll angle, and yaw rate are roughly equal. The output of the controller is considered as the input of the steering system of the autonomous vehicle, which has a low value for both road frictions due to the high longitudinal velocity of vehicle. The ratio of values of rear steering angle to front steering angle is appropriate. If this ratio become higher than this, due to the high longitudinal velocity and critical maneuver, the possibility of unstability exists. Therefore, in addition to lyapanov stability analysis, this ratio indicates a suitable performance of the proposed controller. The presence of variations in the steering angle indicates the efforts of the controller to minimize the lateral position and orientation errors. The control strategy presented in this paper, which employs two parallel controllers, is applicable to control a real 4WS autonomous vehicle.

[Insert Figure 6]

Conclusions

In this paper, an adaptive sliding mode controller has been designed to track the path of an autonomous 4WS vehicle. The controller strategy of this system includes parallel controlling of position and orientation errors of the vehicle. The simplified bicycle model was employed as a plant model for control development purposes. Also, for the purpose of simulation of control strategy, the non-linear full vehicle model has been employed. In addition, with the help of defining Lyapunov functions, the stability of the system has been examined. The results of simulation of this controller show favorable tracking of the path for two different road condition ($\mu = 1$ and $\mu = 0.1$). Considering the stability analysis based on the Lyapanov theorem, the proposed controller is able to resist against parameter variations such as velocity and friction variations and the uncertainties resulting from non-linear model. Further researches can focus on addressing external disturbances, such as crosswinds, analyzing simultaneous longitudinal and lateral performance of the vehicle, using a fuzzy boundary layer to reduce the controlling signal, eliminate the chattering, and increase the accuracy of uncertainties, and applying the controller to a real time system.

References

[1] F. Fahimi, "Full drive-by-wire dynamic control for four-wheel-steer all-wheel-drive vehicles," *Vehicle System Dynamics,* vol. 51, pp. 360-376, 2013.

[2] J. Sridhar and H. Hatwal, "A comparative study of four wheel steering models using the inverse solution," *Vehicle System Dynamics,* vol. 21, pp. 1-18, 1992.

[3] L. Palkovics, "Effect of the controller parameters on the steerability of the four wheel steered car," *Vehicle System Dynamics,* vol. 21, pp. 109-128, 1992.

[4] A. HIGUCHI and Y. SAITOH, "Optimal control of four wheel steering vehicle," *Vehicle System Dynamics,* vol. 22, pp. 397-410, 1993.

[5] Y. H. Cho and J. Kim, "Design of optimal four-wheel steering system," *Vehicle System Dynamics,* vol. 24, pp. 661-682, 1995.

[6] L. Huashi, "Integrated rear wheel steering angle and yaw moment optimal control of four-wheel-steering vehicle," in *2010 Chinese Control and Decision Conference*, 2010, pp. 2490-2493.

[7] L. Gianone, L. Palkovics, and J. Bokor, "Design of an active 4WS system with physical uncertainties," *Control Engineering Practice,* vol. 3, pp. 1075-1083, 1995.

[8] S.-S. You and Y.-H. Chai, "Multi-objective control synthesis: an application to 4WS passenger vehicles," *Mechatronics,* vol. 9, pp. 363-390, 1999.

[9] Z. Rong-hui, C. Guo-ying, W. Guo-qiang, J. Hong-guang, and C. Tao, "Robust optimal control technology for four-wheel steering vehicle," in *2007 International Conference on Mechatronics and Automation*, 2007, pp. 1513-1517.

[10] M. Canale and L. Fagiano, "Stability control of 4WS vehicles using robust IMC techniques," *Vehicle System Dynamics,* vol. 46, pp. 991-1011, 2008.

[11] Z. Civelek, M. Lüy, E. Çam, and N. Barışçı, "Control of Pitch Angle of Wind Turbine by Fuzzy Pid Controller," *Intelligent Automation & Soft Computing,* vol. 22, pp. 463-471, 2016.

[12] R. Sharma, V. Kumar, P. Gaur, and A. Mittal, "An adaptive PID like controller using mix locally recurrent neural network for robotic manipulator with variable payload," *ISA transactions,* vol. 62, pp. 258-267, 2016.

[13] R. Marino, S. Scalzi, and F. Cinili, "Nonlinear PI front and rear steering control in four wheel steering vehicles," *Vehicle System Dynamics,* vol. 45, pp. 1149-1168, 2007.
[14] R. Marino and F. Cinili, "Input–output decoupling control by measurement feedback in four-wheel-steering vehicles," *IEEE Transactions on Control Systems Technology,* vol. 17, pp. 1163-1172, 2009.
[15] R. Marino and S. Scalzi, "Asymptotic sideslip angle and yaw rate decoupling control in four-wheel steering vehicles," *Vehicle System Dynamics,* vol. 48, pp. 999-1019, 2010.
[16] R. Kazemi, M. K. Bahaghighat, and K. Panahi, "Yaw moment control of four wheel steering vehicle by fuzzy approach," in *Industrial Technology, 2008. ICIT 2008. IEEE International Conference on*, 2008, pp. 1-7.
[17] z. j. Wang shufeng, "The Research and Application of Fuzzy Control in Four-wheel-steering Vehicle," presented at the 2010 Seventh International Conference on Fuzzy Systems and Knowledge Discovery (FSKD 2010), 2010.
[18] S. Wu, E. Zhu, M. Qin, H. Ren, and Z. Lei, "Control of Four-Wheel-Steering Vehicle Using GA Fuzzy Neural Network," in *Intelligent Computation Technology and Automation (ICICTA), 2008 International Conference on*, 2008, pp. 869-873.
[19] K. Wakamatsu, Y. Akuta, M. Ikegaya, and N. Asanuma, "Adaptive yaw rate feedback 4WS with tire/road friction coefficient estimator," *Vehicle System Dynamics,* vol. 27, pp. 305-326, 1997.
[20] T. Shiotsuka, A. Nagamatsu, and K. Yoshida, "Adaptive control of 4WS system by using neural network," *Vehicle System Dynamics,* vol. 22, pp. 411-424, 1993.
[21] S. Horiuchi, N. Yuhara, and A. Takei, "Two degree of freedom/H∞ controller synthesis for active four wheel steering vehicles," *Vehicle System Dynamics,* vol. 25, pp. 275-292, 1996.
[22] T. Akita, K. Satoh, and M. C. Gaunt, "Development of 4WS Control Algorithm for a SUV," SAE Technical Paper 0148-7191, 2002.
[23] M. Li and Y. Jia, "Decoupling control in velocity-varying four-wheel steering vehicles with H∞ performance by longitudinal velocity and yaw rate feedback," *Vehicle System Dynamics,* vol. 52, pp. 1563-1583, 2014.
[24] M. Li and Y. Jia, "Precompensation decoupling control with H∞ performance for 4WS velocity-varying vehicles," *International Journal of Systems Science,* pp. 1-12, 2016.
[25] P. I. Ro and H. Kim, "Improvement of high speed 4-WS vehicle handling performance by sliding mode control," in *American Control Conference, 1994*, 1994, pp. 1974-1978.
[26] M. Akar and J. C. Kalkkuhl, "Lateral dynamics emulation via a four-wheel steering vehicle," *Vehicle System Dynamics,* vol. 46, pp. 803-829, 2008.
[27] T. Hiraoka, O. Nishihara, and H. Kumamoto, "Automatic path-tracking controller of a four-wheel steering vehicle," *Vehicle System Dynamics,* vol. 47, pp. 1205-1227, 2009.
[28] A. Alfi and M. Farrokhi, "Hybrid state-feedback sliding-mode controller using fuzzy logic for four-wheel-steering vehicles," *Vehicle System Dynamics,* vol. 47, pp. 265-284, 2009.
[29] F. Du, J.-s. Li, L. Li, and D.-h. Si, "Robust control study for four-wheel active steering vehicle," in *Electrical and Control Engineering (ICECE), 2010 International Conference on*, 2010, pp. 1830-1833.
[30] J. Tian, N. Chen, J. Yang, and L. Wang, "Fractional order sliding model control of active four-wheel steering vehicles," in *Fractional Differentiation and Its Applications (ICFDA), 2014 International Conference on*, 2014, pp. 1-5.
[31] M. Koh, M. Norton, and S. Khoo, "Robust Fault-Tolerant Leader-Follower Control of Four-Wheel Steering Mobile Robots Using Terminal Sliding Mode," *Australian Journal of Electrical and Electronics Engineering,* vol. 9, pp. 247-253, 2012.
[32] B. Li, H. Du, and W. Li, "Fault-tolerant control of electric vehicles with in-wheel motors using actuator-grouping sliding mode controllers," *Mechanical Systems and Signal Processing,* vol. 72, pp. 462-485, 2016.
[33] A. Norouzi, R. Kazemi, and S. Azadi, "Vehicle lateral control in the presence of uncertainty for lane change maneuver using adaptive sliding mode control with fuzzy boundary layer,"

Proceedings of the Institution of Mechanical Engineers, Part I: Journal of Systems and Control Engineering, p. 0959651817733222, 2017.
[34] A. Nizard, B. Thuilot, R. Lenain, and Y. Mezouar, "Nonlinear Path Tracking Controller for Bi-Steerable Vehicles in Cluttered Environments," *IFAC-PapersOnLine*, vol. 49, pp. 19-24, 2016.
[35] J. Ackermann, "Robust decoupling, ideal steering dynamics and yaw stabilization of 4WS cars," *Automatica*, vol. 30, pp. 1761-1768, 1994.
[36] B. Yang, M. Wan, and Q. Sun, "Control strategy for four-wheel steering vehicle handling stability based on partial decoupling design," in *Computational Science and Optimization (CSO), 2010 Third International Joint Conference on*, 2010, pp. 265-267.
[37] M. Li, Y. Jia, and F. Matsuno, "Attenuating diagonal decoupling with robustness for velocity-varying 4WS vehicles," *Control Engineering Practice*, vol. 56, pp. 49-59, 2016.
[38] J. Ackermann, *Robust control: Systems with uncertain physical parameters*: Springer Science & Business Media, 2012.
[39] R. Rajamani, *Vehicle dynamics and control*: Springer Science & Business Media, 2011.
[40] V. I. Utkin, "Sliding mode control design principles and applications to electric drives," *IEEE transactions on industrial electronics*, vol. 40, pp. 23-36, 1993.
[41] J.-J. E. Slotine and W. Li, *Applied nonlinear control* vol. 199: prentice-Hall Englewood Cliffs, NJ, 1991.
[42] O. Barambones, A. Garrido, F. Maseda, and P. Alkorta, "An adaptive sliding mode control law for induction motors using field oriented control theory," in *2006 IEEE Conference on Computer Aided Control System Design, 2006 IEEE International Conference on Control Applications, 2006 IEEE International Symposium on Intelligent Control*, 2006, pp. 1008-1013.
[43] G. Tagne, R. Talj, and A. Charara, "Design and Comparison of Robust Nonlinear Controllers for the Lateral Dynamics of Intelligent Vehicles," *IEEE Transactions on Intelligent Transportation Systems*, vol. 17, pp. 796-809, 2016.

Appendix I- Coefficient of vehicle 2-DOF motion equations

$$a_{11} = -2\mu\frac{c_f + c_r}{mV_x} \qquad a_{21} = 2\mu\frac{l_r c_r - l_f c_f}{JV_x}$$

$$a_{12} = 2\mu\frac{c_f + c_r}{m} \qquad a_{22} = 2\mu\frac{l_f c_f - l_r c_r}{J}$$

$$a_{13} = 2\mu\frac{l_r c_r - l_f c_f}{mV_x} \qquad a_{23} = -2\mu\frac{c_f l_f^2 + c_r l_r^2}{JV_x}$$

$$b_{11} = 2\mu\frac{c_f}{m} \qquad b_{21} = 2\mu\frac{l_f c_f}{J}$$

$$b_{12} = 2\mu\frac{c_r}{m} \qquad b_{22} = 2\mu\frac{l_r c_r}{J}$$

$$d_1 = 2\mu\frac{l_r c_r - l_f c_f}{mV_x} - V_x \qquad d_2 = -2\mu\frac{c_f l_f^2 + c_r l_r^2}{JV_x}$$

Appendix II- Upper and lower bounds of uncertainties for controller design

$$f_1 = A_{11}\dot{e}_1 + a_{12}e_2 + a_{13}\dot{e}_2 + b_{12}u_r + d_1\dot{\psi}_d$$

$$f_1^+ = A_{11}^+\dot{e}_1 + a_{12}^+e_2 + a_{13}^+\dot{e}_2 + b_{12}^+u_r + d_1^+\dot{\psi}_d$$

$$f_1^- = A_{11}^-\dot{e}_1 + a_{12}^-e_2 + a_{13}^-\dot{e}_2 + b_{12}^-u_r + d_1^-\dot{\psi}_d$$

$$\hat{f}_1 = \frac{f_1^+ + f_1^-}{2} = \hat{A}_{11}\dot{e}_1 + \hat{a}_{12}e_2 + \hat{a}_{13}\dot{e}_2 + \hat{b}_{12}u_r + \hat{d}_1\dot{\psi}_d$$

$$\left|f_1^+ - \hat{f}_1\right| = \left|\bar{A}_{11}\dot{e}_1 + \bar{a}_{12}e_2 + \bar{a}_{13}\dot{e}_2 + \bar{b}_{12}u_r + \bar{d}_1\dot{\psi}_d\right| \le F_1$$

$$F_1 = \left|\bar{A}_{11}\dot{e}_1 + \bar{a}_{12}e_2 + \bar{a}_{13}\dot{e}_2 + \bar{b}_{12}u_r + \bar{d}_1\dot{\psi}_d\right|$$

$$f_2 = a_{21}\dot{e}_1 + a_{22}e_2 + A_{23}\dot{e}_2 + b_{21}u_f + d_2\dot{\psi}_d$$

$$f_2^+ = a_{21}^+\dot{e}_1 + a_{22}^+e_2 + A_{23}^+\dot{e}_2 + b_{21}^+u_f + d_2^+\dot{\psi}_d$$

$$f_2^- = a_{11}^-\dot{e}_1 + a_{12}^-e_2 + A_{13}^-\dot{e}_2 + b_{21}^-u_f + d_2^-\dot{\psi}_d$$

$$\hat{f}_2 = \frac{f_2^+ + f_2^-}{2} = \hat{a}_{21}\dot{e}_1 + \hat{a}_{22}e_2 + \hat{A}_{23}\dot{e}_2 + \hat{b}_{21}u_f + \hat{d}_2\dot{\psi}_d$$

$$\left|f_2^+ - \hat{f}_2\right| = \left|\bar{a}_{21}\dot{e}_1 + \bar{a}_{22}e_2 + \bar{A}_{23}\dot{e}_2 + \bar{b}_{21}u_f + \bar{d}_2\dot{\psi}_d\right| \le F_2$$

$$F_2 = \left|\bar{A}_{11}\dot{e}_1 + \bar{a}_{12}e_2 + \bar{a}_{13}\dot{e}_2 + \bar{b}_{12}u_f + \bar{d}_1\dot{\psi}_d\right|$$

$$a_{ij}^+ = a_{ij}(\mu_2) \qquad b_{ij}^+ = b_{ij}(\mu_2)$$

$$a_{ij}^- = a_{ij}(\mu_1) \qquad b_{ij}^- = b_{ij}(\mu_1)$$

$$\hat{a}_{ij} = \frac{a_{ij}^+ + a_{ij}^-}{2} \qquad \hat{b}_{ij} = \sqrt{b_{ij}^+ b_{ij}^-}$$

$$\bar{a}_{ij} = a_{ij}^+ - \hat{a}_{ij} \qquad \bar{b}_{ij} = b_{ij}^+ - \hat{b}_{ij}$$

$$d_i^+ = d_i(\mu_2) \qquad A_{11} = a_{11} + \lambda_1$$

$$d_i^- = d_i(\mu_1) \qquad A_{23} = a_{23} + \lambda_2$$

$$\hat{d}_i = \frac{d_i^+ + d_i^-}{2} \qquad \hat{A}_{11} = a_{11} + \lambda_1$$

$$\bar{d}_i = d_i^+ - \hat{d}_i \qquad A_{23} = a_{23} + \lambda_2$$

$$A_{11} = a_{11} + \lambda_1$$

$$A_{23} = a_{23} + \lambda_2$$

$$\gamma = \sqrt{\frac{b_{22}^+}{b_{22}^-}} = \sqrt{\frac{\mu_2}{\mu_1}} \qquad \gamma = \sqrt{\frac{b_{11}^+}{b_{11}^-}} = \sqrt{\frac{\mu_2}{\mu_1}}$$

$$b_{22}^{-} \le b_{22} \le b_{22}^{+}$$

$$b_{22}^{+} \le \hat{b}_{22} \le b_{22}^{-}$$

$$\sqrt{\frac{b_{22}^{-}}{b_{22}^{+}}} \le b_{22}\hat{b}_{22}^{-1} \le \sqrt{\frac{b_{22}^{+}}{b_{22}^{-}}}$$

$$\gamma^{-1} \le b_{22}\hat{b}_{22}^{-1} \le \gamma$$

$$-\gamma^{-1} \ge -b_{22}\hat{b}_{22}^{-1} \ge -\gamma$$

$$\left|1 - b_{22}\hat{b}_{22}^{-1}\right| \le |1-\gamma^{-1}|$$

$$-\gamma^{-1} \ge -b_{22}\hat{b}_{22}^{-1}$$

$$b_{11}^{-} \le b_{11} \le b_{11}^{+}$$

$$b_{11}^{+} \le \hat{b}_{11} \le b_{11}^{-}$$

$$\sqrt{\frac{b_{11}^{-}}{b_{11}^{+}}} \le b_{11}\hat{b}_{11}^{-1} \le \sqrt{\frac{b_{11}^{+}}{b_{11}^{-}}}$$

$$\gamma^{-1} \le b_{11}\hat{b}_{11}^{-1} \le \gamma$$

$$-\gamma^{-1} \ge -b_{11}\hat{b}_{11}^{-1} \ge -\gamma$$

$$\left|1 - b_{11}\hat{b}_{11}^{-1}\right| \le |1-\gamma^{-1}|$$

$$-\gamma^{-1} \ge -b_{11}\hat{b}_{11}^{-1}$$

Figure Captions List

Table Caption List

Table 1:

Symbol	Variable name	Value	Unit
μ	Road friction coefficient	$[\mu_1\text{-}\mu_2]$	-
M	Mass	1421	[kg]
J	Yaw moment of inertia	2570	[kg.m^2]
l_f	Front axle-COG distance	1.195	[m]
l_r	Rear axle-COG distance	1.513	[m]
C_f	Cornering stiffness of front tire	170550	[N/rad]
C_r	Cornering stiffness of rear tire	137844	[N/rad]

Table 2:

Pavement type	Coefficient of adhesion	Nominal Value
Dry	0.9-1.2	1.05
Wet	0.5-0.89	0.695
Snow	0.2-0.49	0.345
Ice	0.01-0.19	0.1

Figure 1:

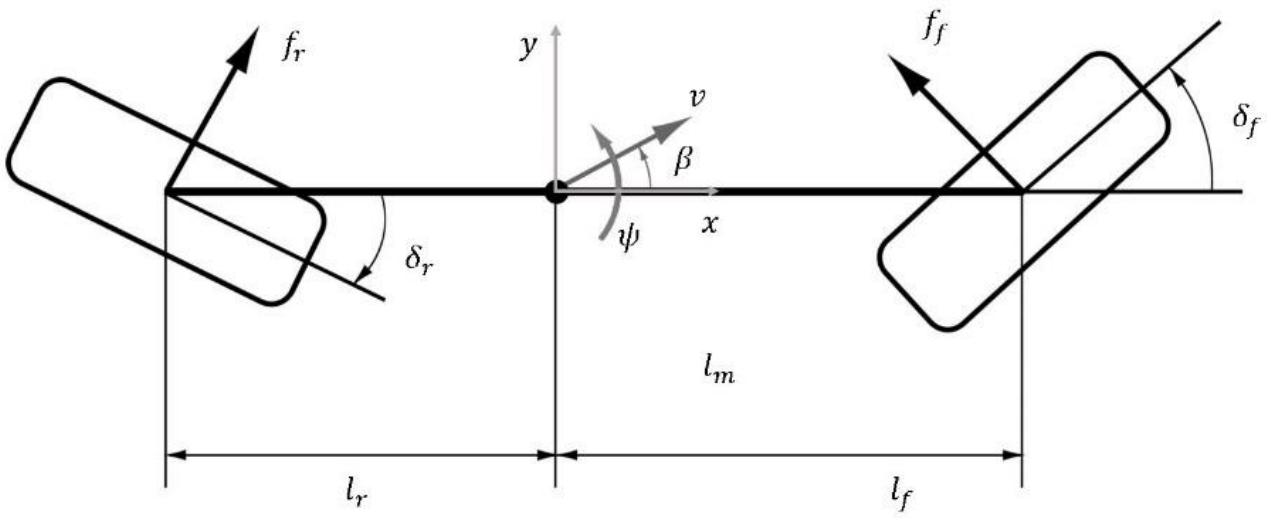

Figure 2:

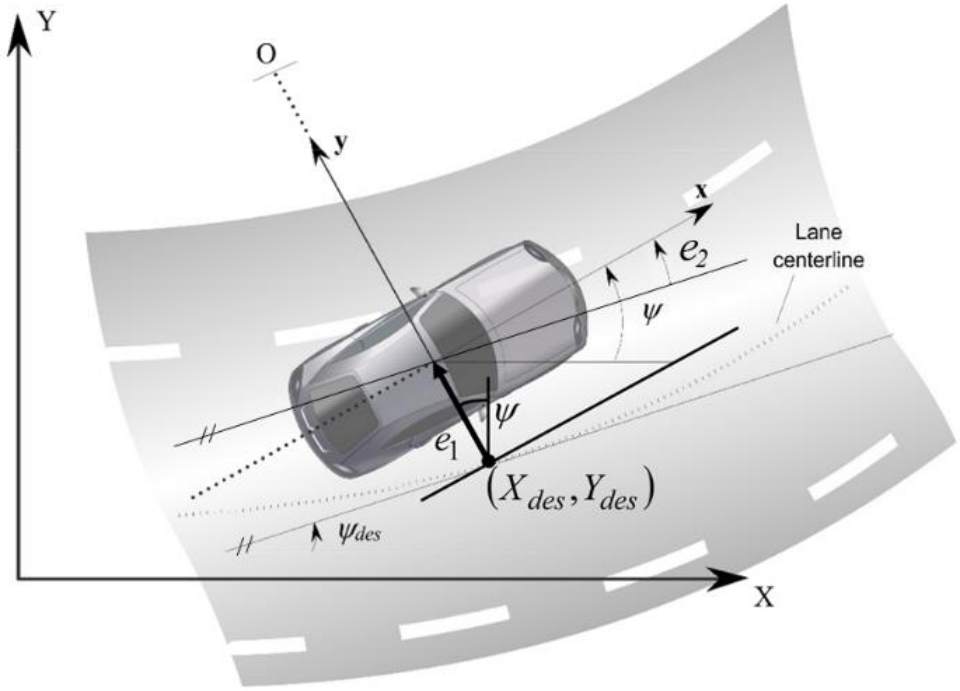

Figure 3:

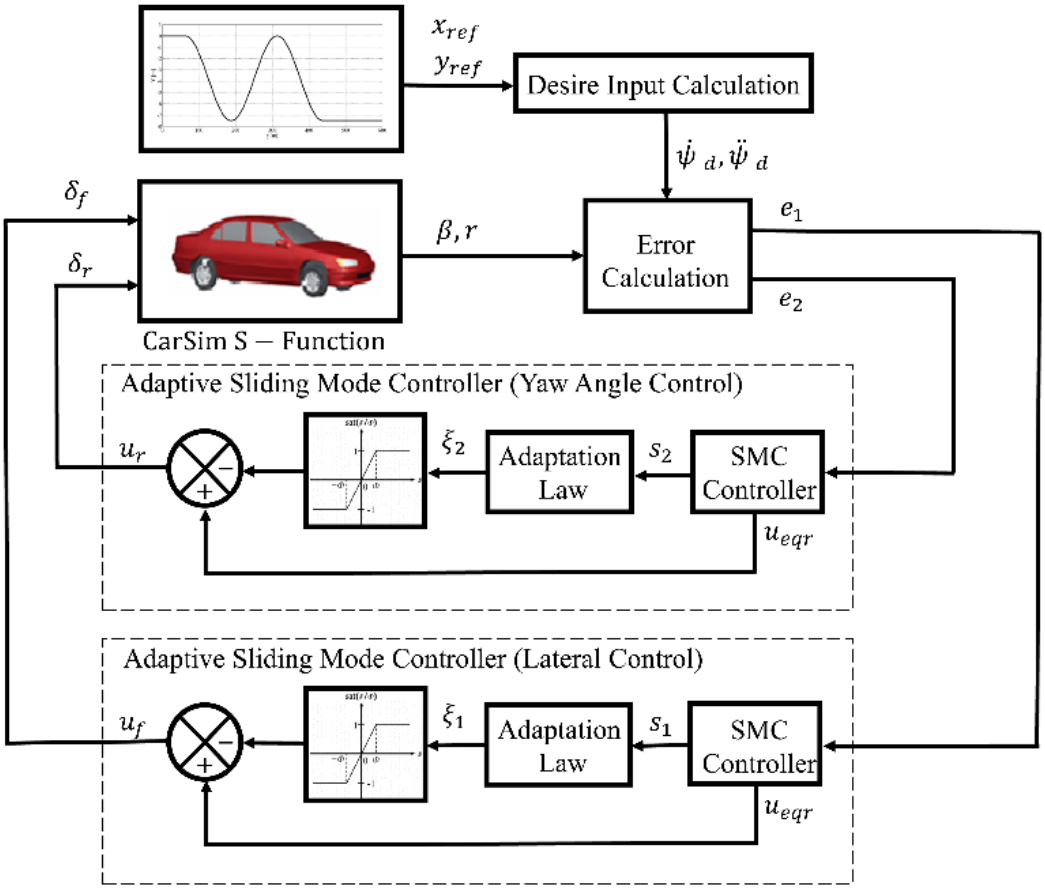
x_{ref}
y_{ref}
Desire Input Calculation
$\dot{\psi}_d, \ddot{\psi}_d$
δ_f
δ_r
β, r
Error Calculation
e_1
e_2
CarSim S – Function
Adaptive Sliding Mode Controller (Yaw Angle Control)
u_r
ξ_2
Adaptation Law
s_2
SMC Controller
u_{eqr}
Adaptive Sliding Mode Controller (Lateral Control)
u_f
ξ_1
Adaptation Law
s_1
SMC Controller
u_{eqr}

Figure 4:

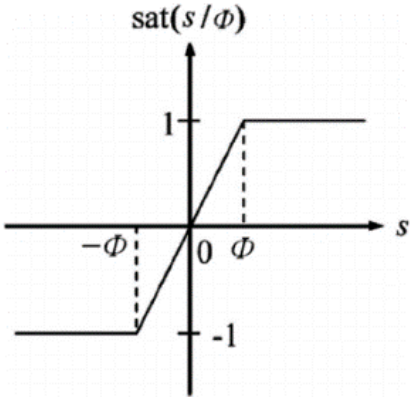

Figure 5:

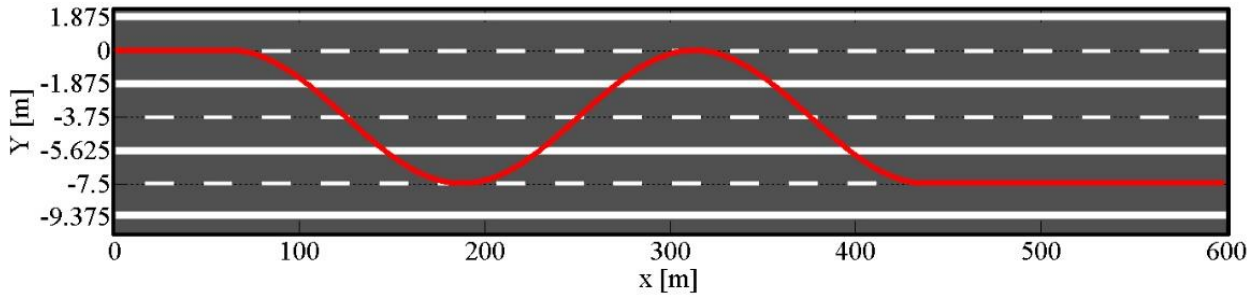

Figure 6:

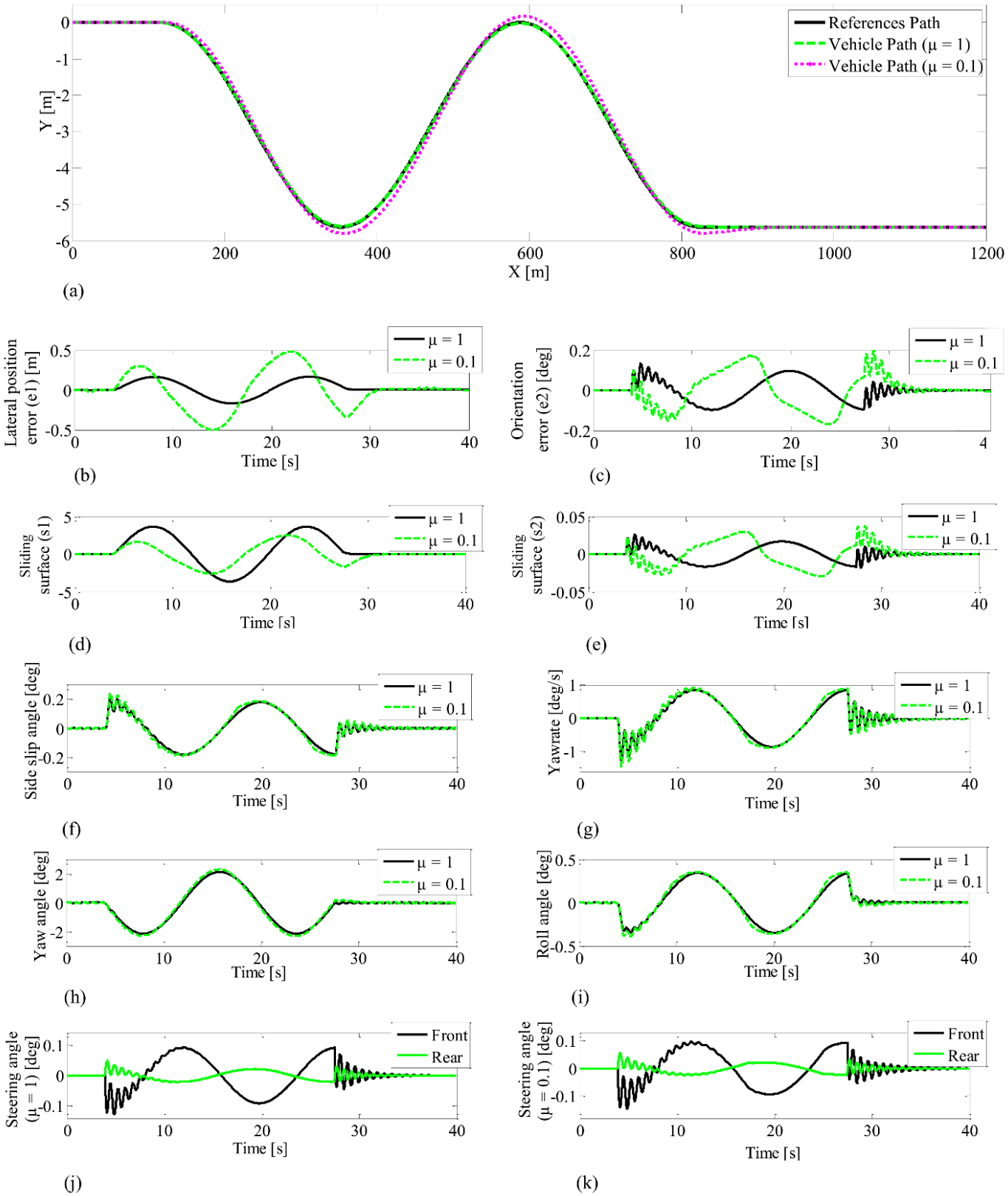
References Path
Vehicle Path (μ = 1)
Vehicle Path (μ = 0.1)
Y [m]
X [m]
(a)
Lateral position error (e1) [m]
Time [s]
(b)
Orientation error (e2) [deg]
Time [s]
(c)
Sliding surface (s1)
Time [s]
(d)
Sliding surface (s2)
Time [s]
(e)
Side slip angle [deg]
Time [s]
(f)
Yawrate [deg/s]
Time [s]
(g)
Yaw angle [deg]
Time [s]
(h)
Roll angle [deg]
Time [s]
(i)
Steering angle (μ = 1) [deg]
Front
Rear
Time [s]
(j)
Steering angle (μ = 0.1) [deg]
Front
Rear
Time [s]
(k)